Asian Journal of Science and Applied Technology
ISSN: 2249-0698 (P) Vol.6, No.2, 2017, pp.28-34

DOI: https://doi.org/10.51983/ajsat-2017.6.2.988

Effects of Radiation and Viscous Dissipation on Transient Free Convection Heat Transfer Flow Past a Hot Vertical Surface in Porous Media

B. Prabhakar Reddy[1*] and P.V. Kanaka Rao[2]

Department of Mathematics, Department of Physics,
College of Natural & Mathematical Sciences, The University of Dodoma, Dodoma, Tanzania
[*]Department of Mathematics, Geethanjali College of Engineering & Technology,
Cheeryal (V), Keesara (M), Medchal, Telangana, India
E-Mail: prabhakar.bijjula@gmail.com
(Received 3 July 2017; Revised 22 July 2017; Accepted 10 August 2017; Available online 18 August 2017)

***Abstract* - The radiation effects on unsteady transient free convection flow of a viscous incompressible gray, absorbing-emitting but non-scattering, optically-thick fluid occupying a semi-infinite porous regime adjacent to an infinite moving hot vertical plate with constant velocity taking viscous dissipation onto account has been carried out. Thermal radiation effects are simulated via a radiation-conduction parameter (K_r), based on the Rossseland diffusion approximation. We employ a Darcian viscous flow model for the porous medium. The momentum and thermal boundary layer equations are non-dimensionalzed using appropriate transformations and then solved subject to physically realistic boundary conditions using the Ritz finite element method. The computed numerical results for velocity (u), temperature (θ), shear stress function (τ) and wall temperature gradient function (Nu) are presented through the graphs and tables for air $(P_r = 0.71)$ and water $(P_r = 7.00)$. It has been found that increasing thermal radiation parameter (K_r) causes a considerable increase in the flow velocity u. Temperature θ is significantly increased within the boundary layer with a rise in K_r. The velocity is found to decrease with an increase in inverse permeability parameter (K_p) and increases with increase in the Grashof number (G_r) and Eckert number (E_c).**

***Keywords:* Free convection, heat transfer, radiation-conduction parameter, hot vertical plate, porous medium.**

I. INTRODUCTION

Radiative-convective heat transfer flows find numerous applications in glass manufacturing, furnace technology, high temperature aerodynamics, fire dynamics, spacecraft re-entry, chemical and ceramics processing. Chung et. al [1] have studied the effects of radiation heat transfer on free convection regime enclosures , with application in geophysics and geothermal reservoirs. In the context of spacecraft technology Sutton [2] as early as suggested that for temperatures ranging from 3500 degrees Fahrenheit to 7000 Fahrenheit, as encountered in rocket propulsion, thermal radiation can account for up to 25% of the total heat transfer. In the internal boundary layer regimes, on rocket combustion thrust chamber walls, significant radiation heat transfer is imparted from the hot propellant to the chamber walls. Hill and Petersen [3] have highlighted the dependence of radiation heat transfer on chamber size dimensions. Chamkha [4] has presented the thermal radiation and buoyancy effects on hydro-magnetic flow over an accelerating permeable surface with heat source or sink. Ganesan and Loganadan [5] have presented the radiation and mass transfer effects on flow of an incompressible viscous fluid past a moving cylinder. Radiation effects on MHD mixed free-forced convective flow past a semi-infinite moving vertical plate for high temperature differences presented by Azzam [6]. Takhar et. al [7] have studied mixed radiation-convection boundary layer flow of an optically dense fluid along a vertically flat plate in a non-Darcian porous medium. Ghosh and Beg [8] have presented theoretical analysis of radiative effects on transient free convection heat transfer past a hot vertical surface in porous media by considering a Darcian viscous flow model for the porous medium. Mohamoud [9] has presented thermal radiation effect on unsteady MHD free convection flow past a vertical plate with temperature dependent viscosity. Chandrakala and Raj [10] have presented the radiation effects on flow past an impulsively started infinite isothermal vertical plate. Here, the fluid is considered a gray, absorbing-emitting radiation but non-scattering medium. Shanker et. al [11] have studied the radiation and mass transfer effects on unsteady MHD free convective fluid flow embedded in a porous medium with heat generation/absorption by finite element method. Bear [12] has presented an excellent treatment of Darcian hydro-magnetics, which is valid for viscous-dominated flows generally to a Reynolds number of about 10. Kaviany [13] has provided an excellent appraisal of Darcian thermal convection flows and also coupled convective-radiative heat transfer in porous media.

Viscous mechanical dissipation effects are important in geophysical flows and also in certain industrial operations and are usually characterized by Eckert number. Gebhart [14] studied the importance of viscous dissipative heat in a free convection flow in the case of isothermal and constant heat flux at the plate. Gebhart and Molledorf [15] presented the effects of viscous dissipation for external natural convection flow over a surface. Viscous dissipation heat on the two dimensional unsteady free convective flow past an infinite vertical porous plate when the temperature oscillates in time and there is constant suction at the plate was studied by Soundalgekar [16]. Computational analysis of coupled radiation-convection dissipation non-gray gas flow in a non-Darcy porous medium using the Keller-Box implicit difference scheme with applications in geothermal energy systems was presented by Takhar et.al [17]. Cookey et. al [18] studied the Influence of viscous dissipation and radiation on unsteady MHD free convection flow past an infinite heated vertical plate in a porous medium with time dependent suction. Zueco [19] studied radiation and viscous dissipation effects on MHD unsteady free convection flow over vertical porous plate by network simulation method. Recently, Reddy [20] studied mass transfer effects on an unsteady MHD free convective flow of an incompressible viscous dissipative fluid past an infinite vertical porous plate by finite element method.

The aim of the present paper is to investigate the radiation effects on unsteady transient free convection flow of a viscous incompressible gray, absorbing-emitting but non-scattering, optically-thick fluid occupying a semi-infinite porous regime adjacent to an infinite moving hot vertical plate with constant velocity by taking viscous dissipation into account. The momentum and thermal boundary layer equations are non-dimensionalized using appropriate transformations. The problem is governed by the system of non-linear partial differential equations, whose exact solutions are difficult to obtain, whenever possible. So that, the Ritz finite element method has been adopted for its solution, which is more economical from a computational point of view. The behaviors of the velocity, temperature, shear stress function and wall temperature gradient function for air and water have been discussed for variations in the governing parameters.

II. MATHEMATICAL MODEL

A two dimensional unsteady flow of a viscous incompressible gray, absorbing-emitting but non-scattering, optically-thick fluid occupying a semi-infinite region of the space past an infinite hot vertical plate moving upwards with constant velocity embedded in a porous medium, as presented in Fig.1. The coordinate system is taken such that the $x'-$ axis is directed along the plate from the leading edge in the vertically upward direction and the $y'-$ axis is normal to the plate. The radiation heat flux in the $x'-$ direction is considered negligible in comparison to the $y'-$ direction. Gravity acts in the opposite direction to the positive $x'-$ axis. The porous regime assumed to be in local thermal equilibrium and thermal dispersion effects are ignored. All the fluid properties are considered constant except the influence of density variation in the body force term under the Oberbeck-Boussineq approximation. The unsteady boundary layer equations of mass, Momentum and energy (heat) conservation under these approximations, neglecting the convective inertial terms, are of the form:

$$\frac{\partial u'}{\partial x'}+\frac{\partial v'}{\partial y'}=0 \tag{1}$$

$$\frac{\partial u'}{\partial t'}=\nu\frac{\partial u'}{\partial y'}+g\beta\left(T'-T'_{\infty}\right)-\frac{\nu u'}{K} \tag{2}$$

$$\frac{\partial T'}{\partial t'}=\frac{k_1}{\rho C_p}\frac{\partial^2 T'}{\partial y'^2}-\frac{1}{\rho C_p}\frac{\partial Q_r}{\partial y'}+\frac{\nu}{C_p}\left(\frac{\partial u'}{\partial y'}\right)^2 \tag{3}$$

The appropriate boundary conditions at the wall and in the free stream are:

$$\begin{aligned}
&u'=0,\quad T'=T'_{\infty}\quad \text{for } y'\geq 0,\ t'\leq 0:\\
&u'=U,\quad T'=T'_{w}\quad \text{for } y'=0,\ t'>0:\\
&u'=0,\quad T'\to T'_{\infty}\quad \text{for } y'\to\infty
\end{aligned} \tag{4}$$

where u' is the velocity component along the plate, v' is the velocity component normal to the plate, g is acceleration due to gravity, ν is the kinematic coefficient of viscosity, T' is temperature of the fluid, T'_{∞} is the temperature of the fluid far away from the plate (in the free stream), ρ is the density, C_p is specific heat at constant pressure, k_1 is the thermal conductivity, β is volumetric coefficient of thermal expansion, t' is the dimensional time, q_r is radiative heat flux, K is the permeability of the porous medium (dimensions, m^2), T'_w is the temperature at the plate and U is the velocity of the moving plate.

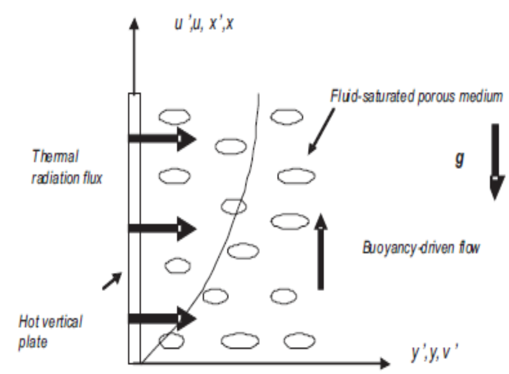

Fig.1 Physical model and coordinate system

The radiation flux on the basis of Rosseland diffusion model for the radiation heat transfer is expressed as;

$$q_r=-\frac{4\sigma^*}{3k^*}\frac{\partial T'^4}{\partial y'} \tag{5}$$

where σ^* is the Stefan-Boltzmann constant and k^* is the spectral mean absorption coefficient of the medium. It is assumed that the temperature differences within the flow are sufficient small such that T'^4 can be expressed as the linear function of temperature T'. It can be established by expanding T'^4 in a Taylor series about a free stream temperature T'_∞ and neglecting higher-order terms, we obtain

T'^4 as

$$T'^4 \cong 4T'^3_\infty T' - 3T'^4_\infty \tag{6}$$

By using equations (5) and (6), equation (3) reduces to

$$\frac{\partial T'}{\partial t'} = \frac{k_1}{\rho C_p}\frac{\partial^2 T'}{\partial y'^2} + \frac{1}{\rho C_p}\frac{4\sigma^*}{3k^*}\frac{\partial^2 T'}{\partial y'^2} + \frac{\nu}{C_p}\left(\frac{\partial u'}{\partial y'}\right)^2 \tag{7}$$

To present solutions which are independent of the geometry of the flow regime, we introduce a series of non-dimensional transformations, defined as:

$$u = \frac{u'}{U}, y = \frac{Uy'}{\nu}, t = \frac{U^2 t'}{\nu}, \theta = \frac{T' - T'_\infty}{T'_w - T'_\infty}, P_r = \frac{\mu C_p}{k_1}, K_p^2 = \frac{\nu^2}{KU^2},$$
$$E_c = \frac{U^2}{C_p(T'_w - T'_\infty)}, G_r = \frac{g\beta\nu(T'_w - T'_\infty)}{U^3}, K_r = \frac{16\sigma T'^3_\infty}{3k^\bullet k_1}. \tag{8}$$

The continuity equation is satisfied and equations (2) and (7) are transformed to:

$$\frac{\partial u}{\partial t} = \frac{\partial^2 u}{\partial y^2} + G_r\theta - K_p^2 u \tag{9}$$

$$\frac{\partial \theta}{\partial t} = \left(\frac{1+K_r}{P_r}\right)\frac{\partial^2 \theta}{\partial y^2} + E_c\left(\frac{\partial u}{\partial y}\right)^2 \tag{10}$$

where u is the dimensionless velocity in the $x-$ direction, t is the dimensionless time, y is the dimensionless distance, G_r is the Grashof number, K_p is the inverse permeability parameter for the porous medium, θ is the dimensionless temperature, P_r is the Prandtl number, K_r is the radiation-conduction parameter and E_c is the Eckert number.

The corresponding boundary conditions are:

$$\begin{aligned} &u = 0, \quad \theta = 0 \quad \text{for } y \ge 0,\ t \le 0,\\ &u = 1, \quad \theta = 1 \quad \text{for } y = 0,\ t > 0,\\ &u = 0, \quad \theta \to 0 \quad \text{for } y \to \infty \end{aligned} \tag{11}$$

III. SOLUTION OF THE PROBLEM

Equations (9) and (10) are non-linear system of partial differential equations are to be solved under subject to the physically realistic boundary conditions given in equation (11). However, whose exact or approximate solutions are difficult to obtain, whenever possible. So that, the Ritz finite element method has been adopted for its solution, which is more economical from a computational point of view. The Ritz finite element method has been employed extensively by the authors in many challenging heat and mass transfer, biomechanics and metallurgical transport phenomena problems over the past few years. The algorithm for Ritz finite element method can be summarized by the following steps.

1. Division of the whole domain into smaller elements of finite dimensions called "finite elements".
2. Generation of the element equations using variational formulations.
3. Assembly of element equations as obtained in step (2).
4. Imposition of boundary conditions to the equations obtained in step (3).
5. Solution of the assembled algebraic equations.

The assembled equations can be solved by any of the numerical technique viz. Gauss-Seidal iteration method. Here, the boundary condition $y \to \infty$ is approximated by $y_{max} = 10$, which is sufficiently large for the velocity to approach convergence criterion. Numerical solutions for the velocity (u) and temperature (θ) are computed by using $C-$ program. Computations are carried out until the steady state is reached. The steady state solution is assumed to have been reached, when the absolute difference between values of velocity (u) and temperature (θ) at two consecutive time steeps are less than 10^{-5} at all nodal points. To prove the convergence of Ritz finite element method, the computations are carried out by making small changes in time t and $y-$directions. For these slightly changed values, no significant change was observed in the values of velocity (u) and temperature (θ). Hence, we conclude that the Ritz finite element method is convergent and stable.

The shear stress function at the wall is given by $\tau = \left(\frac{du}{dy}\right)_{y=0}$

The temperature gradient function at wall is given by

$$Nu = \left(\frac{d\theta}{dy}\right)_{y=0}$$

IV. RESULTS AND DISCUSSION

In order to get physical insight of the flow regime, we have computed numerical values for dimensionless velocity (u), dimensionless temperature (θ), shear stress function (τ) and surface heat transfer function (Nu) for variations in the material parameters encountered in the problem. The computed numerical results are presented through graphs and tables. These results show the effect of the material parameters on the quantities mentioned. During the computation of numerical results, we have taken the material parameters $K_r = 0.5, 1.0, 1.5,$ $E_c = 0.1, 0.3, 0.5,$ $t = 1.0, 1.5, 2.0,$ $G_r = 5.0, 7.0, 9.0$ and $K_p = 1.0, 1.5, 2.0.$

Fig.2 displays the spatial distribution of the dimensionless temperature (θ) for variations in the radiation-conduction parameter (K_r) at fixed time $t = 1.0$ for air $(P_r = 0.71)$ and water $(P_r = 7.00)$ respectively. An increase in the thermal radiation-conduction parameter is observed strongly increase in temperatures for both air and water throughout the fluid with distance normal to the wall in a porous medium regime. Large K_r values correspond to an increased dominance of thermal radiation over conduction. As such thermal radiation supplements the thermal diffusion and increase the overall thermal diffusivity of the regime since Rosseland diffusion flux model adds radiation conductivity to the conventional thermal conductivity. As a result the temperatures in the porous medium flow are significantly increased. Since the medium is highly absorbing, thermal boundary layer thickness will also be increased. The effects of the Eckert number (E_c) on the spatial distribution of the dimensionless temperature (θ) at time $t = 1.0$ for air $(P_r = 0.71)$ and water $(P_r = 7.00)$ are presented in Fig.3, respectively. It can be seen that an increase in the Eckert number increases the temperature for both air and water throughout the flow regime with distance normal to the wall in a porous medium. Fig.4 depicts the effects of time parameter (t) on the spatial distribution of the dimensionless temperature (θ) for air $(P_r = 0.71)$ and water $(P_r = 7.00)$ respectively. It is observed that an increase in time parameter there is a clearly increase in temperature for both air and water. This trend is maintained at all locations in the flow regime for both air and water.

Fig.5 shows the effects of radiation-conduction parameter K_r on the velocity (u) with distance from the wall for air $(P_r = 0.71)$ and water $(P_r = 7.00)$ at time $t = 1.0$ respectively. The parameter K_r defines the relative conduction of the radiation heat transfer to thermal conduction heat transfer. Large K_r values imply large radiation contribution. In the limit as $K_r \to 0,$ thermal radiation flux contribution vanishes i.e., the regime is free convection with thermal conduction at the wall. In the opposite limit as $K_r \to \infty,$ thermal radiation totally dominates thermal conduction.

Hence, with an increase in $K_r,$ thermal radiation will have a stronger contribution than thermal conduction (the contribution is only equal for both modes of heat transfer when $K_r = 1.0$). It is observed that velocity increase for both air and water with increase in thermal radiation contribution. An interesting feature is observed the velocity rises above the prescribed value near the wall and then falls progressively thereafter. The effects of Eckert number (E_c) on dimensionless velocity (u) with distance normal to the wall for air $(P_r = 0.71)$ and water $(P_r = 7.00)$ at time $t = 1.0$ are presented in Fig.6, respectively. It can be seen that velocity increase with increase in the Eckert number for both air and water. In both the cases velocity rises near the wall and then falls gradually from its maximum to minimum. In Fig.7, we have plotted the effects of buoyancy via the Grashof number (G_r) on the dimensionless velocity with distance normal to the wall for air $(P_r = 0.71)$ and water $(P_r = 7.00)$ at time $t = 1.0$ respectively. It is observed that consistently the velocity u is increased with distance y as Grashof number G_r is increased from 5.0 to 7.0 and then 9.0 for both air and water.

The flow is accelerated due to the enhancement in buoyancy force corresponding to an increase in Grashof number i.e., free convection currents. Positive values of G_r corresponds to cooling of the plate surface by natural convection. Heat is therefore, conducted away from the vertical plate into the fluid which increases temperature and thereby enhances the buoyancy force. For the highest values of G_r (i.e. 7, 9), the velocity over-shoots close to the moving plate (at $y \approx 1.2$) after which, velocity descend smoothly to their lowest values in the free stream. In Fig.8, the velocity distribution u plotted with distance from the wall for various values of the inverse permeability parameter (K_p) for air $(P_r = 0.71)$ and water $(P_r = 7.00)$ at time $t = 1.0$ respectively. As the inverse permeability parameter K_p increases from 1.0 to 1.5 and then 2.0, the velocity u decreases with distance transverse to the wall for both air and water. The parameter K_p defined in equation (8) is inversely proportional to the actual permeability K of the porous medium. The Darcian drag force in the momentum equation viz, $-K_p^2 u$ is therefore directly proportional to K_p. An increase in K_p will therefore increase the resistance of the porous medium (as the permeability physically becomes less with increasing K) which will serve to decelerate the flow and reduce velocity u in both the cases. The velocity profiles decay monotonically for all values of K_p from the maximum near the wall to the minimum in the free stream. The profiles of spatial dimensionless velocity u with distance from the wall for various times (t) for air $(P_r = 0.71)$ and water $(P_r = 7.00)$ are presented in Figs.9, respectively. As time t increase from 1.0 to 1.5 and then to 2.0, we observe that the velocity u increases for both air and water. With time the flow is therefore accelerated in the upward direction. Peak velocity always occurs near the wall owing to the translational of the wall in the upward direction, according to the dimensionless boundary condition imposed.

The numerical data for shear stress function (τ) for variations in the material parameters K_r, E_c, G_r, K_p and t for air $(P_r = 0.71)$ and water $(P_r = 7.00)$ are presented in table 1. It is observed that an increase in the radiation-conduction parameter (K_r), Eckert number (E_c), Grashof number (G_r) and time parameter (t) increases the shear stress function values for both air and water whereas an increase in the inverse permeability parameter (K_p) decreases the shear stress function values for both air and water. Also, it is observed that the shear stress function values less in magnitude for water than air. The numerical data for temperature gradient function (Nu) for variations in the material parameters K_r, E_c and t for air $(P_r = 0.71)$ and water $(P_r = 7.00)$ are presented in table 2. It is observed that the temperature gradient function values increases with increasing radiation-conduction parameter (K_r), Eckert number (E_c) and time parameter (t) for both air and water. Also, we notice that the surface temperature gradient function values are less in magnitude for water than air.

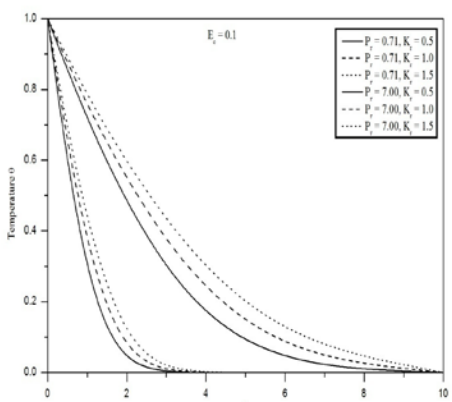

Fig.2 Effect of radiation-conduction parameter (K_r) on the temperature profiles (θ) at $t = 0$.

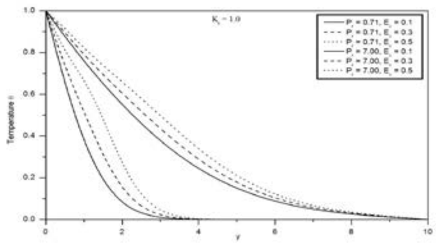

Fig.3 Effect of Eckert number (E_c) on the temperature profiles (θ) at $t = 0$.

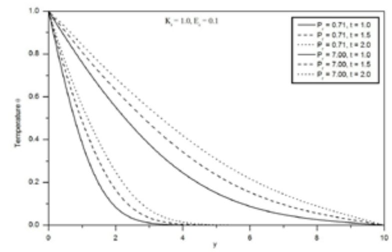

Fig.4 Effect of time parameter (t) on the temperature profiles (θ).

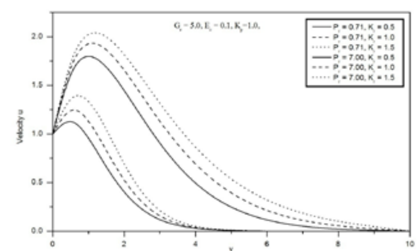

Fig.5 Effect of radiation-conduction parameter (K_r) on the velocity profiles (u) at $t = 0$.

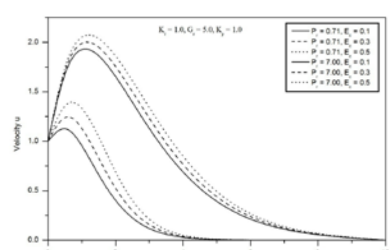

Fig.6 Effect of Eckert number (E_c) on the velocity profiles (u) at $t = 0$.

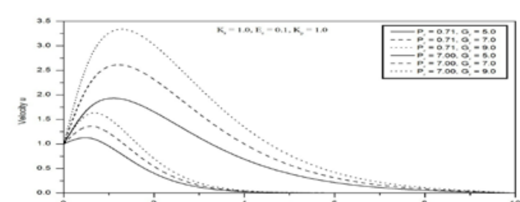

Fig.7 Effect of Grashof number (G_r) on the velocity profiles (u) at $t = 0$.

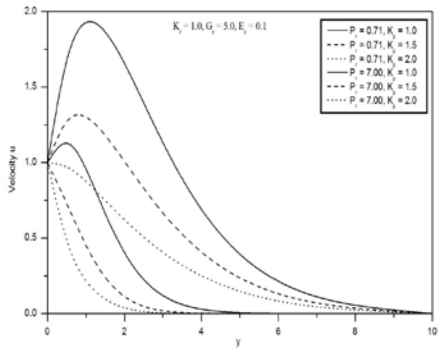

Fig.8 Effect of inverse permeability parameter (K_p) on the velocity profiles (u) at $t = 0$.

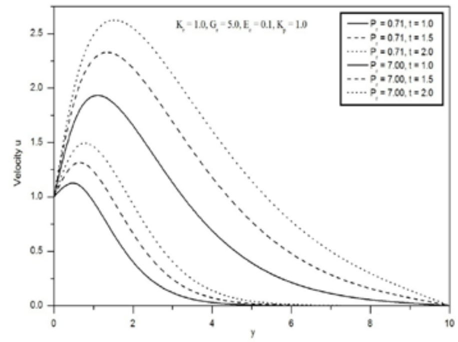

Fig.9 Effect of time parameter (t) on the velocity profiles (u).

TABLE 1 THE NUMERICAL DATA FOR SHEAR STRESS FUNCTION (τ) FOR VARIOUS VALUES OF K_r, E_c, G_r, K_p AND TIME t FOR AIR $(P_r = 0.71)$ AND WATER $(P_r = 7.00)$.

K_r	E_c	G_r	K_p	t	τ for air $(P_r = 0.71)$	τ for water $(P_r = 7.00)$
1.0	0.1	5.0	1.0	1.0	3.541034	2.395702
1.5	0.1	5.0	1.0	1.0	3.644086	2.536740
1.0	0.3	5.0	1.0	1.0	3.607294	2.635066
1.0	0.1	7.0	1.0	1.0	4.512504	2.915658
1.0	0.1	5.0	1.5	1.0	2.650896	1.466172
1.0	0.1	5.0	1.0	1.5	3.922384	2.759292

TABLE 2 THE NUMERICAL DATA FOR TEMPERATURE GRADIENT FUNCTION (Nu) FOR VARIOUS VALUES OF K_r, E_c AND TIME t FOR AIR $(P_r = 0.71)$ AND WATER $(P_r = 7.00)$.

K_r	E_c	t	Nu for air $(P_r = 0.71)$	Nu for water $(P_r = 7.00)$
1.0	0.1	1.0	1.753294	1.289508
1.5	0.1	1.0	1.783700	1.372320
1.0	0.3	1.0	1.791254	1.457414
1.0	0.1	1.5	1.812142	1.421674

V. CONCLUSION

We have been examined the governing equations of the flow for unsteady free convection heat transfer from a vertical translating plate adjacent to a Darcian porous medium in the presence of radiation taking into account viscous dissipation effects. Thermal radiation effects are simulated via a radiation-conduction parameter K_r, based on the Rossseland diffusion approximation. The governing boundary layer equations have been dimensionalized and solved by suing the Ritz finite element method. It has been found that the velocity (u) is increased for both air and water with a rise in the permeability of the porous medium (i.e., a decrease in the inverse permeability parameter (K_p)), with increasing thermal radiation-conduction parameter (K_r), Eckert number (E_c), time (t) and also free convection parameter (G_r). Temperature (θ) is also seen to increase with E_c, t and increasing K_r values for both air and water, owing to an increase in radiation with augments buoyancy in the porous regime. An increase in the inverse permeability parameter reduces in the shear stress function values for air and water. There is a rise in the shear stress function values for air and water with increasing Grashof number and radiation-conduction parameter. Temperature gradient function values increased for air and water by a rise in thermal radiation-conduction parameter, Eckert number and time.

REFERENCES

[1] L. C. Chung, K. T.Yang and J. R. Lloyd, "Radiation-natural convection interactions in two dimensional complex enclosures," ASME J. heat Transfer, Vol. 105, pp.89-95, 1983.

[2] G. P Sutton, *Rocket Propulsion Elements*, New York, John Wiley and Sons, 1956.

[3] P. G. Hill and C. R. Petersen, *Mechanics and Thermodynamics of Propulsion*, 2nd Edition, Addison-Wesley, Reading, Massachusetts, USA, 1967.

[4] A. J. Chamkha, "Thermal radiation and buoyancy effects on hydro-magnetic flow over an accelerating permeable surface with heat source or sink", *Int. J. Eng. Sci*, Vol. 38, pp. 1699-1712, 2000.

[5] P. Ganesan and P. Loganadan, "Radiation and mass transfer effects on flow of an incompressible viscous fluid past a moving cylinder," *Int. J. Heat and Mass Transfer*, Vol. 45, pp. 4281 – 4288, 2002.

[6] G. Azzam, "Radiation effects on the MHD mixed free-forced convective flow past a semi-infinite moving vertical plate for high temperature differences," Physica Scripta, Vol. 66, pp.71-76, 2002.

[7] H. S. Takhar., O. A. Beg., A. J. Chamkha., D. Filip., and I. Pop, "Mixed radiation-convection boundary layer flow of an optically dense fluid along a vertically flat plate in a non-Darcian porous medium," *Int. J. Applied Mechanics and Engineering*, Vol. 8, pp. 483-496, 2003.

[8] K. S. Ghosh and O. A. Beg. "Theoretical analysis of radiative effects on transient free convection heat transfer past a hot vertical surface in porous media," Nonlinear Analysis Modeling and Control, Vol. 13, No.4, pp. 149 – 432, 2008.

[9] M. A. A. Mohamoud. "Thermal radiation effect on unsteady MHD free convection flow past a vertical plate with temperature dependent viscosity," Canadian Journal of Chemical Engineering, Vol.87, pp.441-450, 2009.

[10] P. Chandrakala and S. Antony Raj."Radiation effects on flow past an impulsively started infinite isothermal vertical plate," *Indian J. of Chemical Technology,* Vol.15, pp.63 – 67, 2008.

[11] B. Shanker, B. Prabhakar Reddy and J. Ananad Rao. "Radiation and mass transfer effects on unsteady MHD free convective fluid flow embedded in a porous medium with heat generation/absorption," *Indian J. pure and Applied Physics*, Vol. 48, pp. 157 – 165, 2010.

[12] J. Bear, *Dynamics of Fluids in Porous Media*, Dover, New York, 1998.

[13] M. Kaviany, *Principles of Heat Transfer in Porous Media*, MacGraw-Hill, New York, 1993.

[14] B. Gebhart. "Effects of viscous dissipation in natural convection," J. of Fluid Mechanics, Vol.14, pp.225-232, 1962.

[15] B. Gebhart and J. Mollendorf. "Viscous dissipation in external natural flows," J. of Fluid Mechanics, Vol. 38, pp.79-107, 1969.

[16] V. M. Soundalgekar, "Viscous dissipation effects on unsteady free convective flow past an infinite vertical porous plate with constant suction," *Int. J. Heat and Mass Transfer*, Vol.15, pp. 1253-1261, 1972.

[17] H.S. Takhar., O. A. Beg and M. Kumari, "Computational analysis of coupled radiation-convection dissipation non-gray gas flow in a non-Darcy porous medium using the Keller-Box implicit difference scheme," Int. J. Energy Research, Vol. 22, pp. 141-159, 1998.

[18] C. I. Cookey, A. Ogulu and V. B. Omubo-pepple. "Influence of viscous dissipation and radiation on unsteady MHD free convection flow past an infinite heated vertical plate in a porous medium with time dependent suction," *Int. J. Heat and Mass Transfer*, Vol. 46, pp. 3205-3211, 2003.

[19] J. Zueco Jordan, "Network simulation method applied to radiation and viscous dissipation effects on MHD unsteady free convection over vertical porous plate," *Appl. Mathematical Modeling,* Vol. 31, No.20, pp.2019-2033, 2007.

[20] B. Prabhakar Reddy, "Mass transfer effects on an unsteady MHD free convective flow of an incompressible viscous dissipative fluid past an infinite vertical porous plate," *Int. J. of Applied Mechanics and Engineering*, Vol. 21, No.1, pp.143 – 153, 2016.